At our institute, interstitial hyperthermia is applied for treatment of malignant glioma, particularly with deep-seated tumors or high-risk patients [1-4].

The weak effects of chemotherapy in malignant glioma are generally attributed to ineffective supply of drug to the blood-brain barrier (BBB). However, BBB disruption due to hyperthermia is well known [5-11]. We report two cases of malignant glioma treated with intra-arterial (IA) chemotherapy during hyperthermia, with the expectation of increased adriamycin (ADR) concentration due to disruption of the BBB by hyperthermia.

Materials and Methods

Hyperthermic treatment was planned under computer simulation using a two-dimensional finite element method, as described elsewhere [12].

The interstitial hyperthermia system used in this study was constructed from a 13.56-MHz radio-frequency (RF) generator and needle-shaped electrodes (Fig. 1), as described previously [4]. Heat was generated between an electrode inserted into the tumor and a discoid electrode placed on the chest. Hyperthermic treatment was applied for 60 min.

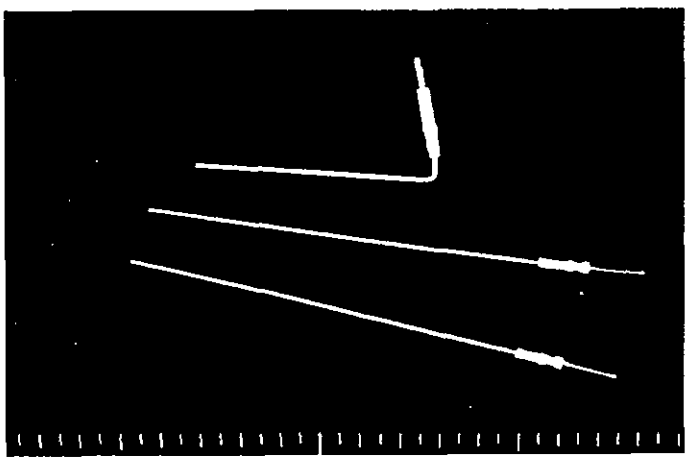

Fig. 1. Needle type electrodes with 1.0 mm diameter for our hyperthermic system.

Case 1 involved a 27-year-old female with local recurrence of right frontal glioma. Histology indicated anaplastic oligoastrocytoma. A cyst was located adjacent to the tumor, and an Ommaya's reservoir had been set in the cyst during a previous surgery (Fig. 2-a).

Case 2 involved a 37-year-old male with recurrent right frontal glioma. Histology was the same as in Case 1. An Ommaya's reservoir positioned in the

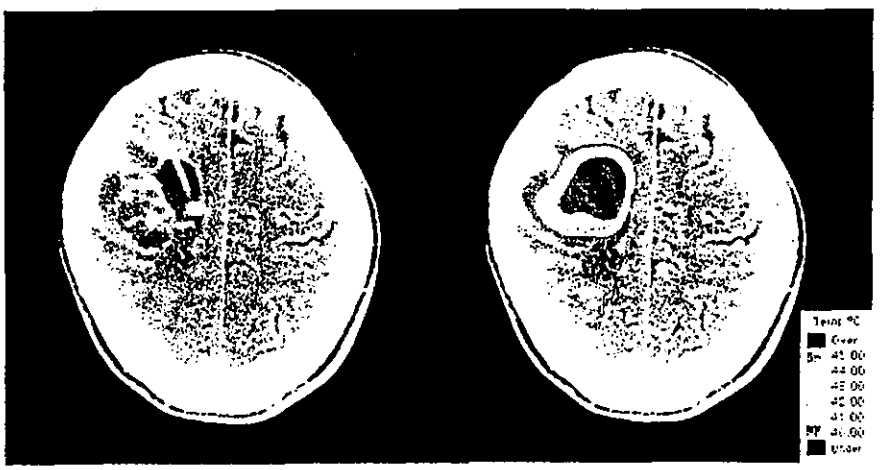

Fig. 2. CT (a) and computer simulation (b) images of case 1. The black dot shows the position of needle-type electrode. The arrow shows the tube of reservoir.

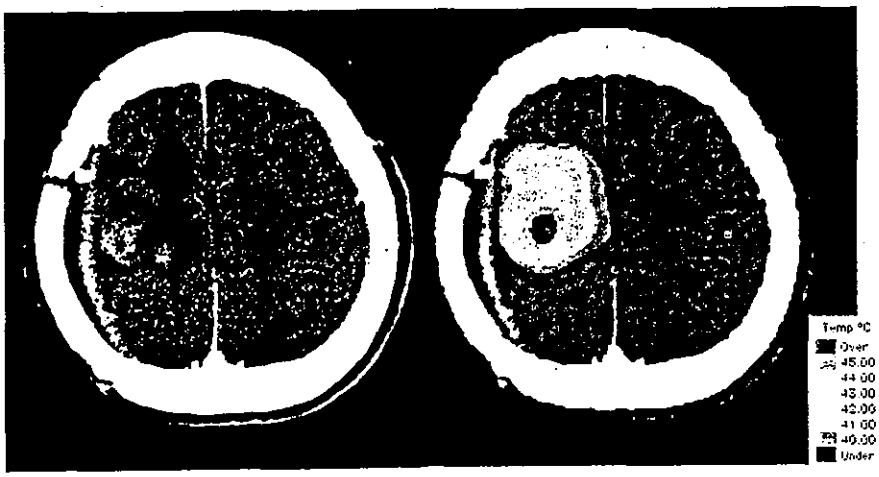

Fig. 3. CT (a) and computer simulation (b) images of case 2. The black dot shows the position of needle-type electrode.

cavity remaining after tumor resection, with recurrent tumor located adjacent to the resection cavity (Fig. 3-a).

In each case, one needle-type electrode was inserted into the preplanned position using stereotactic procedures. After obtaining informed consent, 0.5 mg/kg of ADR was administered via the right common carotid artery over two minutes, and ADR concentration was measured sequentially to determine baseline values. One week later, the same dose of ADR was injected during hyperthermia, and ADR concentrations in the reservoir were sequentially measured by aspiration.

Results

1. *Computer simulation*

Figures 2-b and 3-b show computer simulation images of two cases. Simulation images show thermal distribution extended to the cyst or resection cavity due to reduced blood flow.

2. *ADR concentrations*

In both cases, ADR concentrations in cyst fluid or resection cavity during the second chemotherapy session with heating were higher than those during the first chemotherapy session. In Case 1, maximal ADR concentration was 69.0 ng/ml 30 min after IA injection, compared to 15.5 at baseline (Fig. 4). In Case 2, maximal ADR concentration was 13.3 ng/ml at 60 min after IA chemotherapy, compared to 3.66 ng/ml at baseline (Fig. 5).

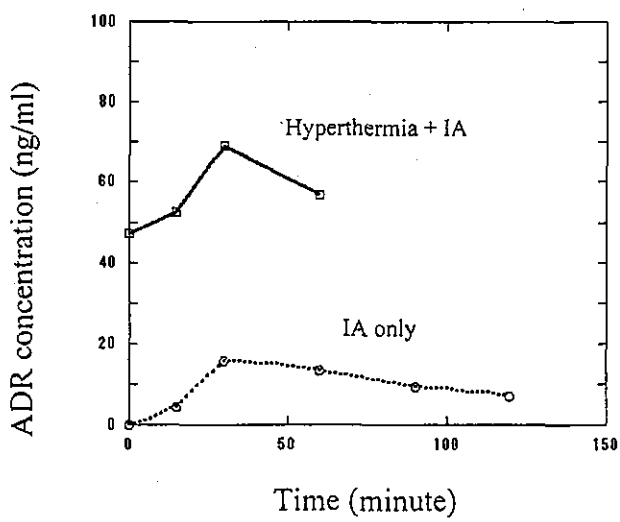

Fig. 4. Serial change of ADR concentration in case 1.

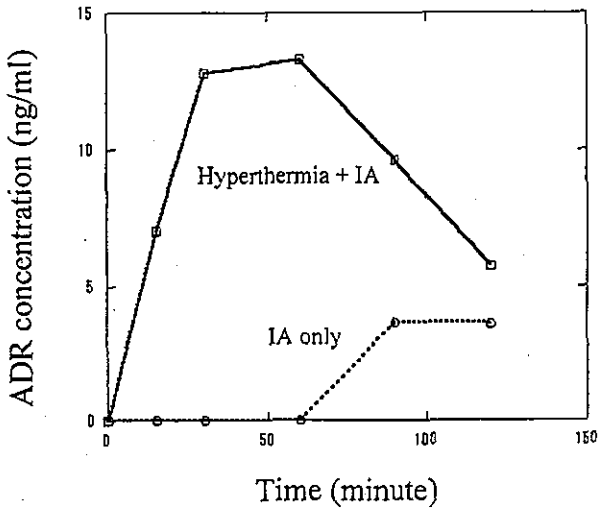

Fig. 5. Serial change of ADR concentration in case 2.

3. *Adverse reactions*

No major adverse reactions, including epileptic seizure, loss of vision, leucoencephalopathy or myelosuppression, were recognized in either case.

4. Efficacy and prognosis

After thermo-chemotherapy, computed tomography (CT) revealed complete response was achieved in Case 1, and stable in Case 2. In Case 1, recurrence was observed 5 months later, and resection was performed. However, 22 months after thermo-chemotherapy, the patient died from multiple bone metastases. In Case 2, regrowth was observed 1 month later, and died 7 months after thermo-chemotherapy.

Discussion

The strategy of our interstitial hyperthermic system is to heat the outer margin of the contrast-enhanced (CE) lesion on CT or magnetic resonance imaging to 42.0-42.5 °C in an eloquent area or 42.5-43.0 °C in a non-eloquent area. Under such conditions, the inside of the CE lesion is above 42.5-43.0 °C, and direct thermal killing of glioma cells is expected. In surrounding brain tissue infiltrated by tumor, the temperature remains below 42.0-42.5 °C during heating. Computer simulation images for the 2 cases in this study showed that the estimated area $\geq$ 43 °C overlapped with the CE lesion and estimated area of 40-42 °C was spread wide around CE lesion considered to be infiltrated by tumor cells (Fig. 2. , Fig. 3.).

With malignant glioma, treatment of tumor invading healthy tissue plays a significant role, as survival depends on controlling local recurrence, and recurrence is often recognized in this area [13-15].

Numerous reports have discussed hyperthermia-induced BBB disruptions [5-11]. Many of these reports, however, concluded that threshold temperatures of $\geq$ 43 °C were required. Ohmoto et al. reported that disruption of the BBB was observed in regions where temperatures reached $\geq$ 43 °C in normal rat brain tissue 10). Ikeda et al. also reported that breakdown of the BBB was observed in normal dog brain heated to 43 °C for 60 min 7). Moriyama et al. reported that extravasation of horseradish peroxidase was observed in rat brain tissue heated to 42.5 °C for 60 min [8].

All these reports were based on normal brain tissues, and reports documenting BBB or tumor-blood barrier disturbance in glioma patients during hyperthermia have been scare. To enhance drug delivery to the tumor invasion zone in the central nervous system, application of mild hyperthermia would be highly desirable.

Cho et al. investigated hyperthermia-induced permeability of BBB using bovine brain microvessel endothelial cells, finding that mild hyperthermia (40 °C for 20 min) can enhance drug penetration through

the BBB 16). Clinical and laboratory studies have also shown that hyperthermia enhances the cytotoxic effects of several chemotherapeutic drugs [17-20]. Among these is ADR, which alone displays dose-dependent cytotoxic effects against glioma cells [19]. These effects are further improved with hyperthermia, even in ADR-resistant cells [21].

The antineoplastic effect of ADR relies on subsequent inhibition of DNA, RNA and protein synthesis. Stan et al. reported that apoptosis could be induced in malignant glioma by ADR if intracellular accumulation reaches cytotoxic levels [22]. Holst et al. studied uptake of ADR in 8 malignant gliomas with intra-venous injection of ADR and reported that tumor tissue concentration of ADR was far below cytotoxic levels [23].

We previously reported the efficacy of combined IA chemotherapy and interstitial hyperthermia in a Wistar rat model [24]. Maximal uptake of ADR in rat C6 glioma was obtained when animals were treated with hyperthermia and IA infusion of ADR. These animals also showed significantly longer overall survival time compared to other treatments.

Technically, IA administration for malignant glioma is easy, due to the anatomical features. The internal and/or vertebral artery feeds the tumor, and both are easily accessible by percutaneous puncture or conventional catheterization. One of the well-known adverse effects of ADR is dose-dependent damage to cardiac muscle. IA chemotherapy offers the advantage of increased uptake during first passage of the drug through tumor vessels, thus reducing total systemic dose and minimizing systemic drug toxicity.

In the two cases described herein, maximal ADR concentration during heating was much higher than that achieved with chemotherapy alone. BBB or blood-tumor barrier disturbance due to hyperthermia was considered the major cause of this increased concentration. However, Cases 1 and 2 displayed substantial variation in ADR concentration despite identical doses. The cyst was located on both sides of the tumor in Case 1, and high temperature was achieved (Fig. 2-b). Conversely, the increase in temperature around the resection cavity was kept mild in Case 2 (Fig. 3-b) to protect the motor area just posterior to the tumor. These factors are probably involved in the differences in ADR concentration. Time to tumor progression was 5 months in Case 1 and 1 month in Case 2. These differences are also of considerable interest.

ADR concentrations in tumor and surrounding brain tissues were not measured in this study, and ADR concentration was not confirmed to reach cytotoxic levels. We are planning further studies to measure ADR concentrations in tumor or tumor invading tissue. IA chemotherapy during hyperthermia is expected to offer effective treatment for malignant glioma, particularly for tumor invading tissue.

References

1) Tanaka R., Kim C. H., Yamada N., Saito Y.: Radiofrequency hyperthermia for malignant brain tumors. Neurosurgery, 17: 114-122, 1987.

2) Takahashi H., Tanaka R., Hondo H., Nakajima T., Watanabe M., Sekihara Y., Kakinuma K.: Clinical experiences of RF hyperthermia for malignant brain tumors. Neurosurgeons, 12: 245-255, 1993. (Japanese).

3) Takahashi H., Tanaka R., Watanabe M., Kakinuma K., Suda T., Takahashi S., Masuda H., Saito A., Nakajima T.: Clinical result of RF interstitial hyperthermia for malignant brain tumors. Japanese J of Hyperthermic Oncology,

11 : 61-67, 1995. (Japanese).

4) Takahashi H., Suda T., Motoyama H., Uzuka T., Takahashi S., Morita K., Kakinuma K., Tanaka R. : Radiofrequency interstitial hyperthermia of malignant brain tumors : Development of heating system. Experimental Oncology, 4 : 186-190, 2000.

5) Shivers R. R., Wijsman J. A. : Blood-brain barrier permeability during hyperthermia. Progress in Brain Research, 115 : 413-424, 1998

6) Nakagawa M., Matsumoto K., Higashi H., Furuta T., Ohmoto T. : Acute effects of interstitial hyperthermia on normal monkey brain - Magnetic resonance imaging appearance and effects on blood-brain barrier -. Neurol. Med. Chir (Tokyo), 34 : 668-675, 1994.

7) Ikeda N., Hayashida O., Kameda H., Ito H., Matsuda T. : Experimental study on thermal damage to dog normal brain. Int. J. Hyperthermia, 10 : 553-561, 1994.

8) Moriyama E., Salcman M., Broadwell R. D. : Blood-brain barrier alteration after microwave-induced hyperthermia is purely a thermal effect : 1. Temperature and Power Measurements. Surg Neurol, 35 : 177-182, 1991.

9) Urakawa M., Yamaguchi K., Tsuchida E., Kashiwagi S., Ito H., Matsuda T. : Blood-brain barrier disturbance following localized hyperthermia in rats. Int. J. Hyperthermia, 11 : 709-718, 1995.

10) Ohmoto Y., Fujisawa H., Ishikawa T., Koizumi H., Matsuda T., Ito H. : Sequential changes in cerebral blood flow, early neuropathological consequences and blood-brain barrier disruption following radiofrequency-induced localized hyperthermia in the rat. Int. J. Hyperthermia, 12 : 321-334, 1996.

11) Sminia P., J. Van Der Zee, Wondergem J., Haveman J. : Effect of hyperthermia on the central nervous system : a review. Int. J. Hyperthermia, 10 : 1-30, 1994.

12) Uzuka T., Tanaka R., Takahashi H., Kakinuma K., Matsuda J., Kato K. : Planning of hyperthermic treatment for malignant glioma using computer simulation. Int. J. Hyperthermia, 17 : 114-22, 2001.

13) Wallner K. E., Galicich J. H., Krol G., Arbit E., Malkin M. G., FRCPC : Patterns of failure following treatment for glioblastoma multiforme and anaplastic astrocytoma. Int. J. Radiation Oncology Biol Phys, 16 : 1405-1409, 1989.

14) Gaspar L. E., Fisher B. J., Macdonald D. R., LeBer D. V., R. T. T. , Halperin E. C., Schold S. C. Jr., Cairncross J. G. : Supratentorial malignant glioma : Patterns of recurrence and implication for external beam local treatment. Int. J. Radiation Oncology Biol Phys, 24 : 55-57, 1992.

15) Sneed P. K., Gutin P. H., Larson D. A., Malec M. K., Phillips T. L., Prados M. D., Scharfen C. O., Weaver K. A., Wara W. M. : Patterns of recurrence of glioblastoma multiforme after external irradiation followed by implant boost. Int. J. Radiation Oncology Biol Phys, 29 : 719-727, 1994.

16) Cho C. W., Liu Y., Cobb W. N., Henthorn T. K., Lillehei K., Christians U., Ng K. Y. : Ultrasound-induced mild hyperthermia as a novel approach to increase drug uptake in brain microvessel endothelial cells. Pharmaceutical Research, 19 : 1123-1129, 2002.

17) Kawai H., Minamiya Y., Kitamura M., Matsuzaki I., Hashimoto M., Suzuki H., Abo S. : Direct measurement of doxorubicin concentration in the intact, living single cancer cell during hyperthermia. Cancer, 79 : 214-219, 1997.

18) Lui R. Y., Matsumoto K., Kunishiro K., Mizumatsu S., Tamiya T., Furuta T., Ohmoto T. : Proliferative potential and apoptosis in rat glioma cell lines after hyperthermia. Neurol Med Chir (Tokyo), 38 : 196-201, 1998.

19) Watanabe M., Tanaka R., Hondo H., Kuroki M. : Effect of antineoplastic agents and hyperthermia on cytotoxicity toward chronically hypoxic glioma cells. Int. J. Hyperthermia, 8 : 131-138, 1992.

20) Schopman E. M., Van Bree C., Kipp J. B., Barendsen G. W. : Enhancement of the effectiveness of methotrexate for the treatment of solid tumours by application of local hyperthermia. Int. J. Hyperthermia, 11 : 561-573, 1995.

21) Asami J., Kawasaki S., Nishikawa K., Kuroda M., Hiraki Y. : Effects of hyperthermia and cepharanthin on Adriamycin accumulation with changes in extracellular pH. Int. J. Hyperthermia, 11 : 27-35, 1995.

22) Stan A. C., Casares S., Radu D., Walter G. F., Brumeanu T. D.: Doxorubicin-induced cell death in highly invasive human gliomas. Anticancer Research, 19: 941-950, 1999.

23) von Holst H., Knochenhauer E., Blomgren H., Collins V. P., Ehn L., Lindquist M., Noren G., Peterson C.: Uptake of Adriamycin in Tumour Surrounding Brain Tissue in Patients with Malignant Gliomas. Acta Neurochi (Wien), 104: 13-16, 1990.

24) Morita K., Tanaka R., Kakinuma K., Takahashi H., Motoyama H.: Combination therapy of rat brain tumours using localized interstitial hyperthermia and intra-arterial chemotherapy. Int. J. Hyperthermia. 19: 204-212, 2003.

研　究

悪性脳腫瘍に対する stereotactic biopsy
－合併症と診断率について－

高橋　英明　　菅井　　努　　宇塚　岳夫　　狩野　瑞穂
本間　順平　　グリニョフ・イゴリ　　田中　隆一

NEUROLOGICAL SURGERY
脳神経外科
（文献略称：No Shinkei Geka）

第32巻　第2号　別刷
2004年2月10日　発行

医学書院

脳神経外科，32(2)：135-140，2004

研究 ◆ *Original Article*

悪性脳腫瘍に対する stereotactic biopsy*
－合併症と診断率について－

高橋　英明**　菅井　努　宇塚　岳夫　狩野　瑞穂
本間　順平　グリニョフ・イゴリ　田中　隆一

Complications and Diagnostic Yield of Stereotactic Biopsy for the Patients with Malignant Brain Tumors

Hideaki TAKAHASHI, Tsutomu SUGAI, Takeo UZUKA, Mizuho KANO, Junpei HONMA, Igor GRINEV, Ryuichi TANAKA

Department of Neurosurgery Brain Research Institute, Niigata University

Purpose: The purpose of this study was to assess the complication risk rate and diagnostic yield in a series of 211 procedures performed by a consistent method at one institute.

Material and method: Two hundred and one patients underwent 211 stereotactic biopsy procedures for diagnosis of malignant brain tumor at Niigata University between 1987-2001. Indication for stereotactic biopsy is decided on the following factors: 1) the patient is elderly or unsuitable for craniotomy; 2) the tumor location is in a deep, diffusing, multiple, eloquent site; 3) cytoreductive surgery is not needed to treat the suspected pathology. The specimen was obtained from the target point of CT scan by the aspiration method under local anesthesia except for in six patients who were children or needed operation for a VP shunt under general anesthesia. The lesion was located in 114 cases of cerebral hemisphere, in 44 cases of basal ganglia, in 11 cases of cerebellum and in 11 cases of spreading site.

Result: Histological diagnosis was obtained in 188 of 211 procedures and the diagnostic yield was 93.5%. There were 104 high grade gliomas, 16 low grade gliomas, 5 germ cell tumors, 37malignant lymphomas, 19 metastatic tumors and 13 negative/inconclusive biopsies. Sixteen patients incurred complications (7.6%). Four patients (1.6%) suffered intratumoral hemorrhage. Emergency craniotomy was performed in three patients and stereotactic aspiration of hematoma was carried out in one patient. Furthermore, of 12 complications, 9 occurred with the patient showing symptoms of worsening neurological deficit, 2 occurred with general convulsion and 1 occurred with severe facial pain.

Conclusion: This study provided evidence that stereotactic biopsy was a safe and reliable tool for patients with unresectable malignant brain tumors.

(Received: July 16, 2003)

Key words stereotactic biopsy, diagnostic yield, complication, and brain tumor

No Shinkei Geka 32(2)：135-140, 2004

Ⅰ．はじめに

悪性脳腫瘍の治療に当たって，組織診断がその治療方針の決定や予後の推定に重要であることは周知のことである[3,4,6]．多くの悪性脳腫瘍において可及的全摘を目指すことが治療において有利であり，また腫瘍の mass effect を減ずる目的から開頭術による生検術が選択されることが多い．しかし，高齢者や performance status の不良例，脳の深部腫瘍，多発性病変といった，開頭術により部分

*(2003. 7. 16 受稿)

**新潟大学脳研究所脳神経外科分野
〔連絡先〕高橋英明＝新潟大学脳研究所脳神経外科（〒951-8585　新潟市旭町通り 1 - 757）
Address reprint requests to: Hideaki TAKAHASHI, M.D., Department of Neurosurgery, Brain Research Institute, Niigata University, 1-757 Asahimachidori, Niigata City, Niigata 951-8585, JAPAN

Fig. 1 A: Raw specimen from stereotoctic biopsy. B: H.E. staining of specimen

ないし全摘出が不可能な症例においては定位脳手術による腫瘍生検術の適応となることも少なくない．stereotactic biopsyを選択するうえでの最大の注目点は合併症率，特に出血率と診断確定率であると考えられる．ことにインフォームドコンセントをするうえで不可欠な情報である．一施設における一定の方法による多数例の報告は，自験例の提示としても他施設との比較においても必要であろう．今回われわれは，臨床診断において悪性脳腫瘍と診断された201例のstereotactic biopsyを経験したので，その成績および合併症について報告する．

Ⅱ．対　象

1987～2001年まで新潟大学医学部附属病院脳神経外科においてCT，MRIにて悪性脳腫瘍を疑われ定位脳手術による生検術が行われた201症例（211回）を対象とした．201症例のうちの10例においては，再発か放射線壊死かの鑑別のためと，再発時に悪性転化が疑われたため2度目のstereotactic biopsyが行われている．12歳以下の小児例とVP shuntを併用した6例以外は局所麻酔下に駒井式CT誘導定位脳手術装置[9]を用いた．生検に用いたプローベは3 mm径の直筒で，CTにて決定したターゲットの直前5 mmのところで内筒を引き抜き，そのままターゲットまで外筒を進める．その際，5 mlのシリンジで2ないし3 ml吸引しつつ外筒を進める．ターゲットにおいて数秒吸引しつつ待ち，その後吸引圧を保ちながらプローベを抜去する．柔らかい腫瘍以外は円筒状に標本が採取される（Fig. 1）．それで採取できないときは，駒井式吸引用プローベを用い採取するが，3カ所以上の採取は行わず終了する．年齢は3～84歳，平均55.4歳で，男性121例，女性80例である．部位は大脳半球114例，基底核44例，小脳11例，多発性17例，び漫性11例であった．術前臨床診断はgerm cell tumor 6例，high grade glioma 107例，low grade glioma 20例，malignant lymphoma 39例，metastatic tumor 20例，その他9例であった．手術直前に局所麻酔下にて頭部に固定したフレームを着けて頭部CTスキャンを施行し，腫瘍中心をターゲットとして設定した．術前にlow grade gliomaを疑われた症例は近接した正常白質も採取するようtrajectoryも設定した．プローベの刺入方向はCTスキャンにて決定しておき，eloquent areaを通らないよう配慮した．最近では，多発性のgliomaや広範に拡がるgliomaにおいては，MRIのdiffusion imageでhigh intensityを示す病巣のところをtargetとしてspecimenを採取している（Fig. 2）．

Ⅲ．結　果

生検により組織を確定し得たのは201例中188例であり，93.5%の診断確定率であった（Table 1）．周辺正常脳組織採取や組織片の不十分採取による診断不能例は13例（6.5%）で，その臨床診断はgerm cell tumor 1例，high grade glioma 3例，low grade glioma 4例，malignant lymphoma 2例，metastatic tumor 1例，その他2例である．その13例の臨床診断，腫瘍局在，組織診断をTable 2に示す．Glioma 128例についてみると，確定診断率は94.5%，診断不能例は7例(5.5%)で

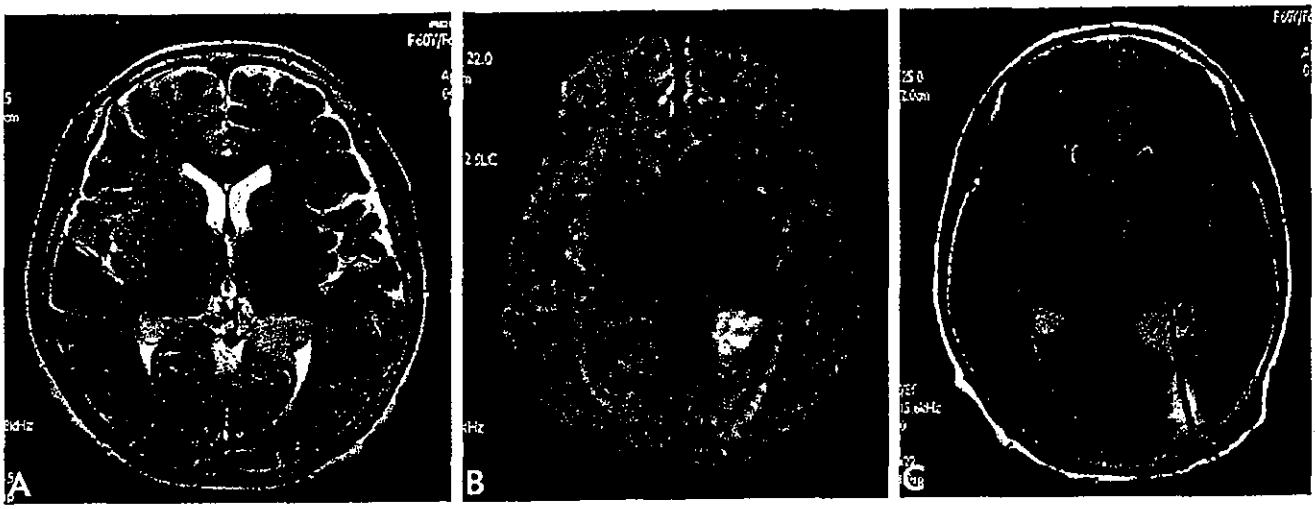

Fig. 2 A : Preoperative MRI images (T2-weighted image). B : Diffusion image of preoperative MRI demonstroted a high intensity area in the tumor. C : Post operative MRI revealed the trajectory of the stereotactic biopsy.

Table 1 Summary of 201 patients with clinical and histological diagnosis

	Clinical	Histological	Diagnostic yield
Germ cell tumor	6	5	83.3%
Glioma	127	120	94.5%
high grade	107	104	97.2%
low grade	20	16	80.0%
Malignant lymphoma	39	37	94.9%
Metastatic tumor	20	19	95.0%
Miscellaneous	9	7	77.8%
		Diagnostic yield 188/201	93.5%

Table 2 Summary of 13 patients with negative result

	Sex/age	Clinical diagnosis	Location	Histological diagnosis
1	5M	germ cell tumor	basal ganglia	normal tissue
2	10F	high grade glioma	brainstem	inadequate tissue
3	78M	high grade glioma	cerebellum	normal tissue
4	61F	high grade glioma	multicentric	inadequate tissue
5	15M	low grade glioma	brainstem	inadequate tissue
6	39M	low grade glioma	frontal	normal tissue
7	30M	low grade glioma	uncus	normal tissue
8	27M	low grade glioma	multicentric	normal tissue
9	51M	malignant lymphoma	basal ganglia	inadequate tissue
10	61M	malignant lymphoma	cerebellum	normal tissue
11	70F	metastatic tumor	basal ganglia	inadequate tissue
12	70M	miscellaneous	frontal	normal tissue
13	72M	miscellaneous	cerebellum	normal tissue

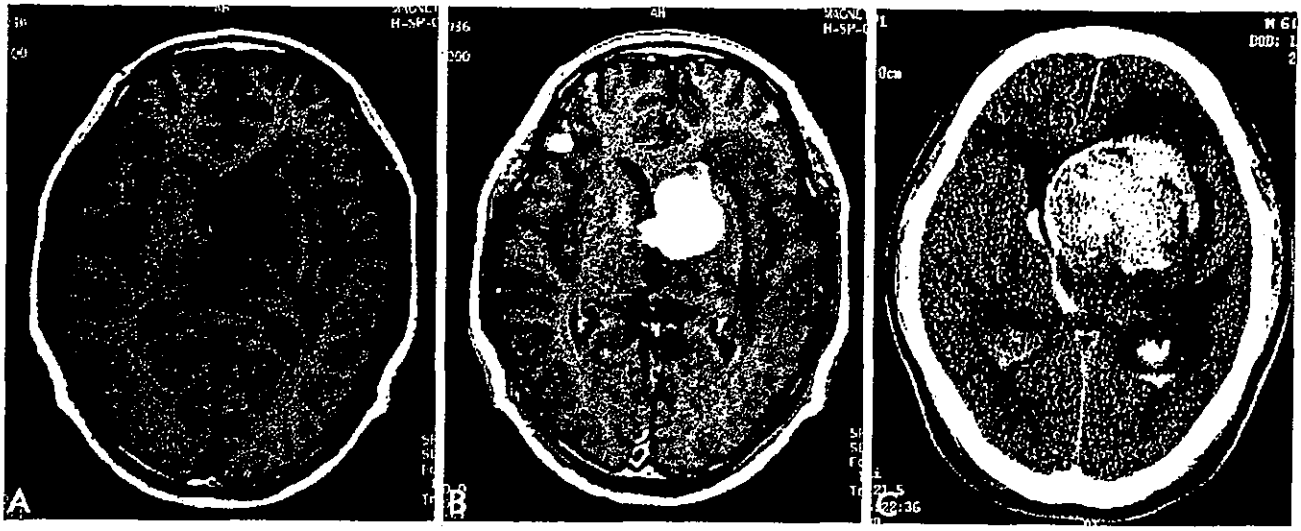

Fig. 3 A : Preoperative MRI image (T1-weighted image). B : Contrast-enhanced T1-weighted image revealed tumor in the left basal ganglia. C : Post operative CT demonstrated intratumoral hemorrhage with brain edema.

Table 3 Grading distinction in gliomas of 127 patients

Distinction	99
No distinction	21
Inadequate tissue	7
	127

あった．Grading が不能な例は，臨床診断の high grade glioma 群で 15 例（14%），low grade glioma 群で 5 例（25%）であった．ただし，high grade glioma のなかで anaplastic astrocytoma と glioblastoma の区別は specimen も小さいことから明確にはつけられなかったこともあり，本研究では言及していない（Table 3）．

合併症としては 211 回中 16 例（7.6%）あり，出血が 4 例（1.9%）に認められた．うち 3 例は開頭術にて血腫除去を，1 例は定位脳手術により血腫吸引を行った．出血例の組織型は glioma 2 例，malignant lymphoma 1 例（Fig. 3）と germinoma 1 例であった．その他の合併症として，痙攣 2 例，術後顔面疼痛 1 例の他，術前症状の悪化が一過性に認められたのが 9 例であった．いずれも画像上浮腫の増強などの変化は認められなかった．その組織型はすべて glioma の症例であった．16 例の詳細は Table 4 に示した．特に腫瘍の組織型，局在，合併症の種類，症状，その治療およびその症状の回復までの時間について示した．

Ⅳ. 考　察

本研究では，一施設における悪性脳腫瘍の stereotactic biopsy による診断確定率とその合併症の頻度について報告した．悪性脳腫瘍の stereotactic biopsy について考えるとき，その採取部位の組織診断の妥当性や採取量の少なさ，盲目的採取によって引き起こされる出血などの合併症などが問題とされる[12,16]．しかし，その前に考えるべき点は stereotactic biopsy の適応であろう．もともと，悪性脳腫瘍では，可及的摘出が予後にも影響することから，stereotactic biopsy が選択される例は特殊であり，単に摘出術と採取量や出血率などの比較はできない．それは，stereotactic biopsy 選択群には，放射線治療を行うためにある程度悪性とわかればよいとか，採取が，容易に吸引し得なければ無理をしないといった症例も少なくないと考えられるからである．一般に適応としては，部位的な観点から全摘困難な深部腫瘍や eloquent area に存在する腫瘍，さらには multiple に存在するものなどがあり，患者側の要因としては高齢者や全身麻酔に対しリスクを有する例などが挙げられる[5,12]．

これまでの stereotactic biopsy の 200 例を超える報告で，合併症としての出血率を示したものは，Bernstein ら[2]がまとめており，0.6～7.2%となっている[1,2,13,14,17-19]．さらに，彼らは biopsy の際の

Table 4 Complications among 211 stereotactic biopsies

No.	Case	Age	Sex	Diagnosis	Location	Complication	Sign	Treatment	Duration
1	YS	13	M	GCT	r-BG	hemorrhage	hemiparesis	operation	3W
2	SW	79	F	HGG	l-O	hemorrhage	hemiparesis	operation	3hr
3	BS	83	M	HGG	L-P	hemorrhage	unconsciousness	operation	1M
4	TH	66	M	ML	l-BG	hemorrhage	unconsciousness	operation	6M
5	KH	49	M	HGG	l-F	convulsion	(−)	no	1hr
6	AM	15	M	HGG	l-BG	convulsion	(−)	no	1hr
7	TS	50	M	HGG	l-T	anopsia	(−)	steroid	4W
8	SA	42	M	HGG	b-F	symptom worsened	hemiparesis	steroid	1W
9	KF	64	M	HGG	multiple	symptom worsened	hemiparesis	no	3d
10	MH	80	F	HGG	l-T	symptom worsened	aphasia	no	5d
11	TH	51	M	HGG	r-BG	symptom worsened	hemiparesis	steroid	cont'd
12	SS	51	M	HGG	l-P	symptom worsened	disorientation	steroid	1W
13	TK	78	M	HGG	r-F	symptom worsened	hemiparesis	steroid	conti'd
14	SK	64	M	HGG	L-P	symptom worsened	Gerstman	steroid	4d
15	SI	76	F	ML	multiple	symptom worsened	hemiparesis	steroid	conti'd
16	CA	78	M	HGG	l-T	facial pain	(−)	steroid	1hr

GCT : germ cell tumor, HGG : high grade glioma, ML : malignant lymphoma, BG : basal ganglio, O : occipital, P : parietal, F : frontal, T : temporal, r : right, l : left, b : bilateral, hr : hour, d : day, W : week, M : month, conti'd : continued

出血の危険因子として，組織像，腫瘍局在，頭蓋内圧亢進症状の有無などを挙げている[2]．組織像では特に，glioma や悪性リンパ腫の易出血性を指摘している[1,2,5,12]．われわれの出血例では，glioma 2 例，malignant lymphoma 1 例 と germinoma 1 例であった．Germinoma は基底核部にあり，組織型というより location の要素が出血に結びついていると考えられた．その他に出血の要因として腫瘍血管の豊富な例を指摘する報告[10,12]もあり，術前の血管撮影も参考にすべきであろう．また，今回の検討では要因として挙がらなかった高血圧の存在も出血の合併に影響することが懸念され，高齢者がこうした stereotactic biopsy の適応となることも少なくなく，高血圧のある場合の対応も心得ておく必要があるかもしれない．

本報告に目立つ transient neurological worsening は，画像上は手術の前後で変化がないものの神経症状が悪化するものである．文献上は脳幹部や白質病変の生検術においてよくみられるとされている[1,13,14,18]が，われわれの例では，すべて glioma であり，局在というより組織型の要因として特徴づけられた．その理由は不明であるが，1 つの要素としては glioma の経過中に生検術が行われ，症状が顕性化する例が含まれることが考えられる．

次に，診断確定率についてであるが，どの報告からも 80〜100% くらいの診断率が出されており[5-8,11,12,15,20]，当科における 93.5% は妥当なところと言える．ただし，当然ながら high grade glioma における anaplastic astrocytoma と glioblastoma を区別することは十分ではないなどの欠点はあり，吸引にて採取できないものも数例存在する．さらに，悪性神経膠腫の heterogeneity についても同様で，われわれの施設でも最近の例では，MRI の diffusion image で採取部位を決定するなど試みているが，SPECT や PET，MR spectroscopy などの併用がより効果的であることは言うまでもない．

最後に，診断し得なかった 13 例についてであるが，腫瘍そのものの要因とテクニカルな部分としての要因に分けて考える必要がある．前者は腫瘍が吸引法にて引けないような性状だとか，すぐに粉砕化してしまうようなものであり，本方法では採取不能なタイプで，この stereotactic biopsy の限界ともいうべき要因である．後者は，CT を含めた機器における誤差，吸引が弱すぎたなどの術者の要素，画像でのターゲットのエラーなどが要因となる．これらは，機器への精通，経験，サンプルエラーをなくすための工夫により診断率を高められる要因でもある．この 13 例のうち，脳幹部 2 例，基底核 4 例，小脳 3 例，側頭葉鉤部 1 例という腫瘍の主座からみても多くのサンプルの採取は

困難であり，テクニカルな要因が多く含まれたと考えられる．

いずれにしても，本法の適応となる条件，状況を考えるならば，本研究におけるわれわれの定位的腫瘍生検術は十分な診断率であると確信する．

V．結　語

当科における定位脳手術による生検術の成績では，確定診断率において94.5%，診断不能率では5.5%であり，合併症は7.6%に認められた．高齢者やリスクファクターの多い症例，深部や広範に拡がった悪性脳腫瘍においては有用な手段と考える．

文　献

1) Appuzo MLJ, Chandrasoma PT, Cohen D, Zee CS, Zelman V: Computed imaging stereotaxy: experience and perspective related to 500 procedures applied to brain masses. Neurosurgery **20**: 930-937, 1987
2) Bernstein M, Parrent AG: Complications of CT guided stereotactic biopsy of intra-axial brain lesions. J Neurosurgery **81**: 165-168,1994
3) Brucher JM: Neuropathological diagnosis with stereotactic biopsies; Possibilities, difficulties and requirements. Acta Neurochir **124**: 37-39, 1993
4) Chandrasoma PT, Smith MM, Apuzzo MLJ: Stereotactic biopsy in the diagnosis of brain masses: Comparison of results of biopsy and resected surgical specimen. Neurosurgery **24**: 160-165,1989
5) Field M, Witham TF, Flickinger JC, Kondziolka D, Lunsford LD: Comprehensive assessment of hemorrhage risks and outcomes after stereotactic brain biopsy. J Neurosurg **94**: 545-551, 2001
6) Greene GM, Hitchon PW, Schelper RL, Yuh W, Dyste GN: Diagnosis yield in CT-guided stereotactic biopsy of gliomas. J Neurosurgery **71**: 494-497,1989
7) Hall WA, Liu H, Martin AJ, Maxwell RE, Truwit CL: Brain biopsy sampling by using prospective stereo taxis and a trajectory guid. J Neurosurgery **94**: 67-71, 2001
8) Hall WA: The safety and efficacy of stereotactic biopsy for intracranial lesions. Cancer **82**: 1749-1755, 1998
9) 駒井則彦：CTを利用した定位脳手術．No Shinkei Geka **14**: 123-133, 1986
10) Kondriolka D, Lunsford LD: The role of stereotactic biopsy in the management of gliomas. J Neuro oncol, **42**: 205-213, 1999
11) Kreth FW, Warnke PC, Sceremet R, Ostertag CB: Surgical resection and radiation therapy versus biopsy and radiation therapy in the treatment of glioblastoma multiforme. J Neurosurgery **78**: 762-766, 1993
12) 松本健五，富田 亨，東久 登，中川 実，芦立 久，多田英二，前田八州彦，大本堯史：脳腫瘍に対するimage guided stereotactic biopsy71 例の経験．No Shinkei Geka **23**: 897-903, 1995
13) Mundinger F: CT stereotactic biopsy for optimizing the therapy of intracranial processes. Acta Neurochir Suppl **35**: 70-74, 1985
14) Ostertag CB, Mennel HD, Kiessling M: Stereotactic biopsy of brain tumors. Surg Neurol **14**: 275-283, 1980
15) Ranjan A, Rajshekhar V, Josepf T, Ghandy MJ, Chandy SM: Nondiagnostic CT-guided stereotactic biopsies in a series of 407 cases: influence of CT morphology and operator experience. J Neurosurgery **79**: 839-844, 1993
16) Revesz T, Scaravilli F, Coutinho L, Cockburn H, Sacrares P, Thomas DGT: Reliability of histological diagnosis including grading in gliomas biopsied by image-guided stereotactic technique. Brain **136**: 781-793, 1993
17) Sawin PD, Hitchon PW, Follet KA, Torner JC: Computed imaging assisted stereotactic brain biopsy. A risk analysis of 225 consecutive cases. Surg Neurol **49**: 640-649, 1998
18) Sedan R, Peragut JC, Farnarier P, Hassoun J, Sethian M: Intra-encephalic stereotactic biopsies (309 patients/318 biopsies). Acta Neurochir Suppl **33**: 207-210, 1984
19) Voges J, Schroeder R, Treuer H, Pastyr O, Schlegel W, Lorenz WJ, Sturm V: CT-guided and computer assisted stereotactic biopsy. Acta Neurochir **125**: 142-149, 1993
20) Wen DY, Hall WA, Miller DA, Selieskog EL, Maxwell RE: Targeted brain biopsy: a comparison of freehand computed tomography-guided and stereotactic techniques. Neurosurgery **32**: 407-413, 1993

Original Article

The Significance of Lipid Resonances in Proton MR Spectroscopy of Brain Tumors

Yasuyuki Yoshida, Katsuyuki Tanaka, and Takuo Hashimoto

聖マリアンナ医科大学雑誌

第32巻　第4号　別刷

(平成16年8月発行)

Original Article

St. Marianna Med. J.
Vol. 32, pp. 329-338, 2004

The Significance of Lipid Resonances in Proton MR Spectroscopy of Brain Tumors

Yasuyuki Yoshida, Katsuyuki Tanaka, and Takuo Hashimoto

(Received for Publication: August 20, 2004)

Abstract

We studied the significance of lipids (Lip) to confirm the effectiveness of proton magnetic resonance spectroscopy (^{1}H-MRS) for brain tumors. Among the cases diagnosed as a brain tumor between April 2003 and June 2004 at our hospital, 24 cases underwent preoperative ^{1}H-MRS. They were all primary cases and confirmed by pathological diagnoses and required surgical extirpation. The obtained specimens underwent ^{1}H-MRS, were analyzed and prepared as frozen sections. All the sections were compared and examined with H&E staining, Ki-67 labeling index (MIB-1 index), and Sudan-II staining. There were 14 out of 24 (58.3%) Lip positive cases in ^{1}H-MRS, and the positive cell rate of Sudan-II staining and MIB-1 indexes were higher in the cases with increased Lip, so it seemed that they indicated a rapid tumor growth rate. In contrast, there were some cases with a high MIB-1 index, no increase in Lip, and a low positive cell rate as seen with Sudan-II staining, so it seemed that they indicated that the tumor growth was detected at a relatively early stage.

With ^{1}H-MRS, although there are problems such as a change of pattern due to settings and precision, it is a useful and valid test to determine the diagnosis and evaluate the grade of malignancy from a metabolic state. Furthermore, in this study, the developmental stage and growth rate of a tumor can be determined by knowing its biological behavior. This study may also be of help in predicting its prognosis and determining its therapeutic effects.

Key Words

proton magnetic resonance spectroscopy, lipid droplets, necrosis, biological behavior, brain tumor

Introduction

Proton-magnetic resonance spectroscopy (^{1}H-MRS) uses the principal of MR and allows surgeons to non-invasively determine the body's metabolic state and is currently employed for various disorders. In neurosurgery, it is used as a supplemental diagnostic tool, the effectiveness and importance of which have been reported with the development of recent imaging techniques. For brain tumors, among other applications, every facility uses it in clinical applications because it allows the preoperative determination of the kind of tumor and whether it is benign or malignant[1-4].

In ^{1}H-MRS for brain tumors, the relative signals of choline (Cho) related to the production and disintegration of cell membranes, creatine (Cr) that is an intermediary product of energy metabolism, *N*-acetyl-aspartate (NAA) that is specifically contained in neurons and neural processes, lactate (Lac) that is a product of anaerobic glycolysis, and lipids (Lip) that are implicated in most pathological changes.[5] Protons and these factors are measured and their patterns enable a correct diagnosis.

Department of Neurosurgery, St. Marianna University School of Medicine, 2-16-1 Sugao, Miyamae-ku, Kawasaki 216-8511, Japan

Though there are many reports on ^{1}H-MRS related to the histological diagnoses of tumors[6,7], there are few reports on the evaluation of grade of malignancy. And most of those reports are related to the Ki-67 labeling index that indicates the grade of histological malignancy and the change of Cho, Cr, and NAA, and those related to Lip are only found occasionally[8-11].

Based on the examination of Lip obtained from ^{1}H-MRS of brain tumors operated on at our hospital, of the 55 cases, the tumors confirmed by pathological diagnoses with more histological malignancy tended to show Lip frequently[12]. In general, there is not so much lipid in brain tissue as to appear in signals on ^{1}H-MRS and its appearance reflects necrosis, and a tumor with more histological malignancy shows signals easily.

The studies on the appearance of lipid in brain tumors are usually carried out with rats[13-15], and there are only a few surgical studies on humans. In this study, we will evaluate the correlation between the implication of the appearance of Lip in ^{1}H-MRS and the grade of biological malignancy and examine its effectiveness.

Methods

Subjects

We studied 24 patients diagnosed as having a brain tumor from April 2003 to June 2004 who underwent preoperative ^{1}H-MRS. They were primary cases and confirmed by histopathological diagnosis and judged to require surgical extirpation, including stereotacitic biopsy. However, the cases with a history of irradiation and the cases undergoing chemotherapy were excluded. Their ages ranged from 2 to 84 years (average age ± standard deviation: 59.8±18.4), including 14 male cases and 10 female cases. Regarding the specimens used in this study, we obtained informed consent for the use of extirpated specimens from the patients or their family. This study was approved by the ethics committee of St. Marianna University Hospital.

Imaging conditions

In MR imaging, Gyroscan NT Intera/Master 1.5 T (Philips Medical Systems) was used, and the MRI was used for routine preoperative T1WI, T2 WI, FLAIR, and Gd-EDTA. The imaging condition of ^{1}H-MRS was as follows: the PRESS (point resolved spectroscopy) method, TR/TE = 2000 ms/136 ms, 3 Hz Gauss function, -1.5 Hz exponential function. A part of the tumor lesion which showed an enhancing effect by Gd-EDTA was measured with a single voxel of 1 to 8 cm^3. If the imaged part is smaller than the voxel, we tried not to include the surrounding normal brain as much as possible and aimed at inside a solid or cystic lesion. Signals were selected as: 3.2 ppm for Cho, 3.0 ppm for Cr, 2.0 ppm for NAA, 1.3 ppm downwards for Lac, 1.3 ppm upwards and 0.9 ppm for Lip (**Fig. 1**). The peak values of each signal were measured, and the two peak values of Lac and Lip were totaled. The Cho/Cr ratio was also calculated. Cho, Cr, NAA, and the Cho/Cr ratio were determined as increasing or decreasing by the comparison of the value of the opposite side. Lac and lip were determined as positive if a signal was confirmed.

Pathological examination

A specimen was extracted from the area of the voxel setting point as close as possible. The specimen was placed in an OTC compound and was frozen and sliced with a cryotome at −20°C at a thickness of 10 μm. Each section was stained with hematoxylin and eosin (H&E), Ki-67 immunostaining, and Sudan-II.

H&E staining: For diagnosis and confirmation of necrosis and its localization.

Ki-67 immunostaining (MIB-1 index): Antihuman GFA mouse monoclonal antibody (DAKO Corp.) was used as a primary antibody, and Ki-67 immunostaining was performed with the LSAB2 (Labeled Streptavidin Biotin 2) method. The positive cell rate of each section, for more than 1,000 cells, was measured to calculate the MIB-1 index.

Sudan-II staining: A tumor cell which stained with red oil stain was regarded as a lipid droplet, and the tumor cells with such droplets were considered as positive. The positive cell rate of each section for more than 1,000 cells was then calculated for the MIB-1 index. Necrotic tissue was excluded from this measurement.

Statistical tests

Data were classified according to pathological diagnosis and analyzed. StatView 5.0 (SAS Institute) was used for data analysis, and the Student's t-test was used to determine the significant differences among each group in which $p<0.05$ was considered significantly different. For the comparison of 2 variables, the Pearson's correlation coefficient was used.

Results

The Lip positive cases in ^{1}H-MRS were 14 cases

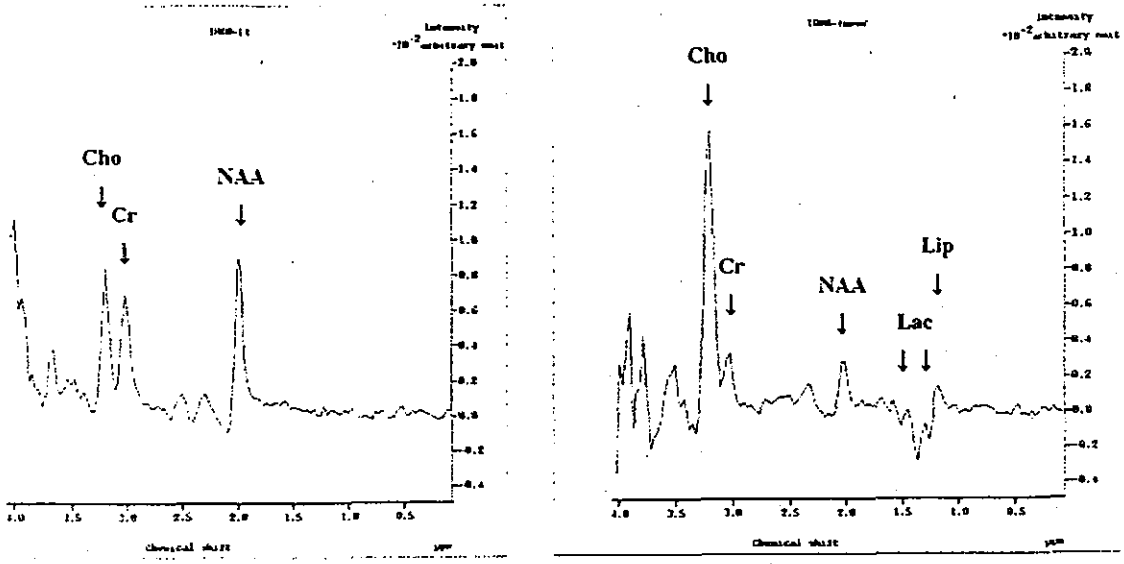

Fig. 1. Typical proton-MR spectra (NO.3: Anaplastic oligoastrocytoma). Right is normal brain tissue. Left is brain tumor. Each resonances are choline-related molecules (Cho) at 3.2 ppm, creatine (Cr) at 3.0 ppm, N-acetyl-aspartate (NAA) at 2.0 ppm, lactate (Lac) at 1.3 ppm and lipid (Lip) at 1.3 and 0.9 ppm. Lac and Lip are not detected in normal brain tissue. Cho is increased, Lac and Lip are revealed in brain tumor.

of 24 (58.3%). Classified by the pathological diagnosis, Lip positive cases were as follows: 7 cases of 11 (63.6%) for malignant brain tumor (WHO classification grade III, grade IV), 2 cases of 2 (100%) for malignant lymphoma, 3 cases of 4 (75%) for metastatic brain tumor, 2 cases of 5 (40%) for meningioma. However, there were no Lip positive cases for pituitary adenoma and acoustic neurinoma (**Table 1**).

The higher the histological malignancy, a higher percentage of lipid droplets stained with Sudan-II appeared in the cells (**Fig. 2**). Necrotic areas were stained with Sudan-II as well as in tumor cells. There were many positive cells adjacent to the necrotic areas (**Fig. 3**).

Correlations were confirmed both between Lip and the positive cell rate of Sudan-II staining, and the positive cell rate of Sudan-II staining and the MIB-1 index ($r=0.49$, $r=0.59$) (**Figs. 4, 5**). Regardless of the necrosis in H&E stained sections and high positive cell rate of Sudan-II staining, there were 5 cases (3 malignant glioma cases, 1 metastatic brain tumor case, and 1 meningioma case) with no increase in Lip. The pathological diagnoses were as follows.

1. Glioblastoma multiforme (WHO classification, grade IV)
   Three cases out of 6 were Lip positive (50%). The 3 cases showed a significantly higher MIB-1 index compared to the other 3 cases ($p<0.05$) (**Fig. 6**).
2. Ganglioneuroblastoma (WHO classification, grade IV)
   Lip positive and both the positive cell rate of Sudan-II staining and the MIB-1 index were high.
3. Anaplastic astrocytoma (WHO classification, grade III)
   Three cases out of 4 were Lip positive (75%). One case (No. 20) with no Lip, showed a ring-like enhancement on the MRI, the Cho/Cr ratio was high as was the MIB-1 index, but the positive cell rate of Sudan-II staining was low.
4. Metastatic brain tumor
   Three cases out of 4 were Lip positive (75%). One case (No. 1) with no Lip was a solid tumor on MRI and showed necrosis in H&E stained sections.
5. Malignant lymphoma (WHO classification, grade IV)
   Both cases were Lip positive. There was no necrosis. Both the positive cell rate of Sudan-II staining and the MIB-1 index were high.
6. Meningioma
   Two cases were Lip positive out of 5 (40%).

Table 1. Summary of Patients and Results

No.	Age	Sex	Diagnosis	WHO class.	MRI ring like enhancement	1H-MRS Cho/Cr	1H-MRS Lip reson. (1/1000)	H-E necrosis	Pathology Sudan-II (%)	Mib-1 (%)
8	55	M	Glioblastoma	IV	(+)	2.04	0.478	(+)	28.7	27.9
17	83	F	Glioblastoma	IV	(+)	–	14.401	(+)	64.2	25.9
21	52	M	Glioblastoma	IV	(+)	2.72	1.229	(+)	24.5	20.9
5	75	M	Glioblastoma	IV	(+)	3.21	-	(+)	24.2	13.7
22	78	M	Glioblastoma	IV	(–)	5.25	-	(+)	31.2	10.7
23	38	M	Glioblastoma	IV	(+)	5.02	-	(+)	19.3	16
11	2	F	Ganglioneuroblastoma	IV	(+)	2.17	1.578	(+)	49.3	19.5
15	76	F	Anaplastic astrocytoma	III	(–)	3.97	0.539	(+)	14.3	11.8
3	59	M	Anaplastic oligoastrocytoma	III	(–)	5.17	1.448	(+)	18.9	17.3
16	56	F	Anaplastic astrocytoma	III	(–)	2.87	1.488	(+)	66	25.6
20	64	F	Anaplastic astrocytoma	III	(+)	17.84	-	(+)	4.9	16.3
6	71	F	Metastatic brain tumor	-	(+)	2.62	3.455	(+)	24.3	28.8
9	54	M	Metastatic brain tumor	-	(+)	–	6.658	(+)	33.6	31.3
19	64	F	Metastatic brain tumor	-	(+)	–	6.272	(+)	15.5	28.8
1	62	M	Metastatic brain tumor	-	(–)	2.37	-	(+)	44.6	39.1
13	71	M	Malignant lymphoma	IV	(–)	–	4.182	(–)	47.8	57.1
24	71	M	Malignant lymphoma	IV	(–)	–	0.395	(–)	12.3	41.8
12	61	F	Meningioma	I	(–)	–	1.451	(–)	5.4	12.7
18	55	F	Meningioma	I	(–)	2.10	0.878	(–)	1.7	0.7
4	71	M	Meningioma	II	(–)	–	-	(+)	4.8	3
7	74	M	Meningioma	I	(–)	–	-	(–)	5.2	4.3
14	73	M	Meningioma	I	(+)	–	-	(–)	9.7	1.8
10	23	M	Pituitary adenoma	I	(–)	–	-	(–)	3.3	3.5
2	47	F	Acoustic neurinoma	I	(–)	–	-	(–)	13.6	7.1

There was no correlation between Sudan-II staining and the MIB-1 index. Both cases with Lip positive (Nos. 12 and 18) showed low values in Sudan-II staining. In contrast, there was one case (No. 4) that showed no Lip but necrosis in H&E staining.

7. Pituitary adenoma and acoustic neurinoma
Two cases showed no Lip and increased only in Cho.

Discussion

There are many reports on ^{1}H-MRS as pathological diagnosis of brain tumors. There are only a few reports on the evaluation of grading of histological malignancy, and most of them have compared the MIB-1 index and the increase in Cho, the decrease in Cr, the increase of the Cho/Cr ratio, the increase of the Cho/NAA ratio, or the appearance of Lac. Reports on the signal of Lip are only occasionally found[6,7,16].

The appearance of Lip in ^{1}H-MRS is usually viewed that it reflects the necrosis of cells. However, imaging enhanced by Gd-EDTA in MRI and the appearance of Lip in areas that are not necrotic indicate the existence of micronecrosis and lipid droplets[6,7,16]. Lipid droplets are lipids absorbed into a cell, which indicates the previous step of necrosis, i.e., the change of metabolism due to inadequate blood flow. Therefore, when lipid droplets are found in tumor cells, they are no doubt malignant cells with a high biological activity and a strong proliferation ability[4]. In the present study, the higher the histological malignancy, the darker the lipid droplets in tumor cell substrate were stained with Sudan-II.

In general, necrosis often occurs in a solid tumor, and tumor vessels are regularly arranged around the necrotic area both *in vitro* and *in vivo*[17]. Moreover, some tumors have vessels at their center and form cylindrical cord-like structures consisting of live cells surrounded by necrotic tissue, or some form a tumor nodule consisting of a central necrotic area and a peripheral network of vessels. Necrosis will occur when the nutrients leak from the tumor vessels and decrease substantially and/or will occur when the toxic cell degradation products increase[18]. Blood stagnation in capillary vessels due to infarction in a tumor may also cause necrosis of a tumor.

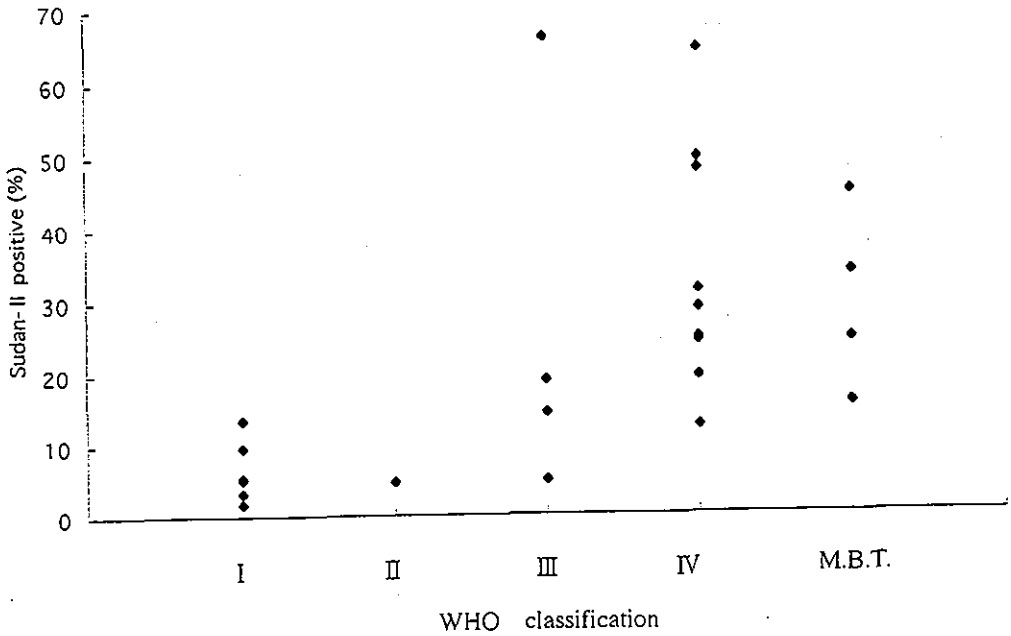

Fig. 2. The comparision of Sudan-II stain positive cells and classified WHO classification is shown.

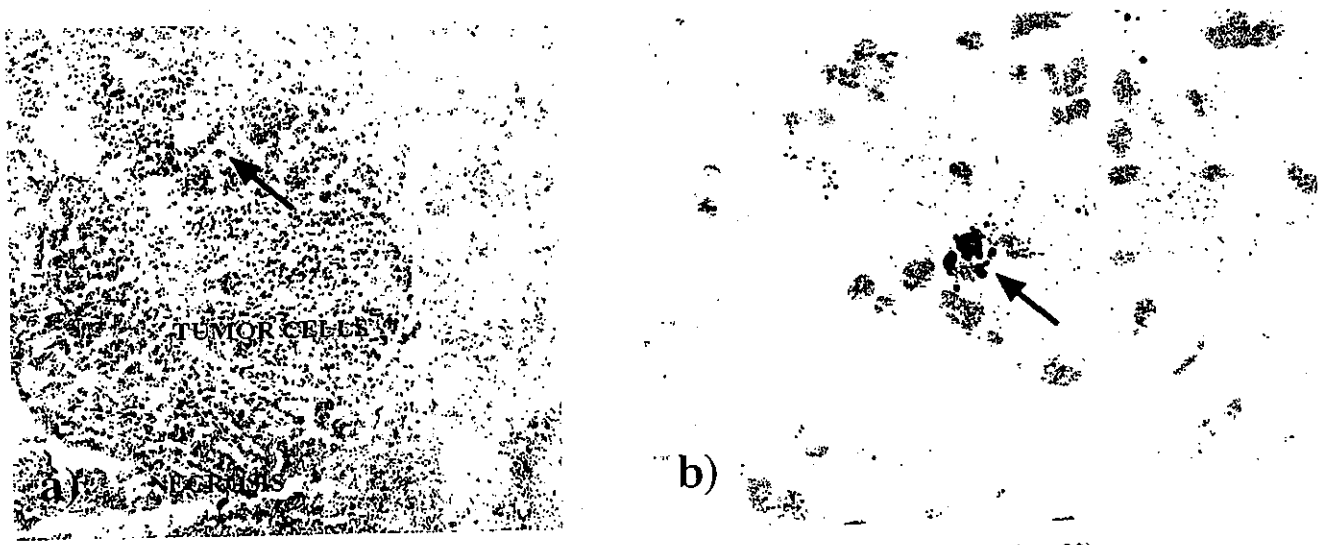

Fig. 3. a) The droplet (indicated by arrows) is shown in the necrotic tissue. (Sudan-II stain×80)
b) The lipid droplet is visible in the tumor cell (indicated by arrows). (Sudan-II stain×400)

The proliferative rate of cells close to a vessel, which are well nourished, is higher than those of tumor cells close to a necrotic area[19]. Some tumors do not become necrotic but instead form a watery cyst. ^{1}H-MRS is a means by which the growth stage and rate of tumors, along with the biological grades of the tumors can be precisely determined.

From the pathological examination at the early stage of tumor growth, it can be said that there is an increase of Cho, and a decrease of Cr and NAA. With further growth of the tumor, a low nutrient and hypoxic state occurs and Lac appears. Moreover, with growth of the tumor, Lip from lipid droplets, micronecrosis, and necrosis appears (Fig. 7 a-c). When the setting of voxel is completely focused on a necrotic portion, Cho, Cr, and NAA will decrease or be eliminated, and the signals will consist of only Lac and Lip, and the findings of a cyst and/or infarction will become similar (Fig.7 c-e).

As if supporting the relation between the bio-

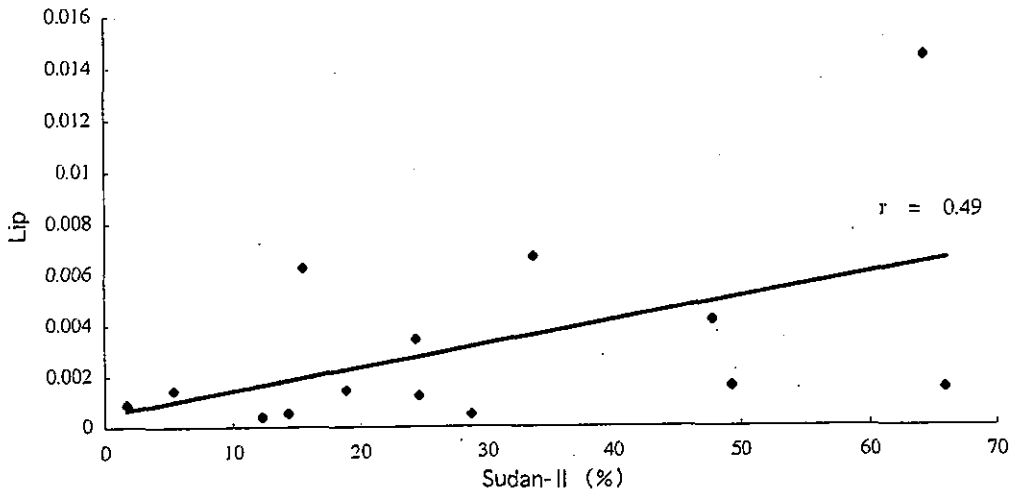

Fig. 4. The relation between lipid resonances (Lip) in ^{1}H-MRS and Sudan-II stain positive cells rate (%) is shown. The correlation coefficient is 0.49.

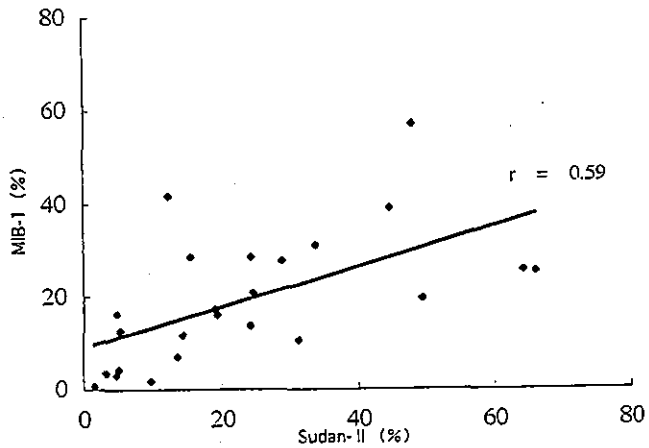

Fig. 5. The correlation between MIB-1 index (MIB-1) and Sudan-II positive cells rate (Sudan-II) is shown. The correlation coefficient is 0.59.

logical grade of malignancy and the appearance of Lip, when the cases were surveyed according to the groups classified by histological diagnosis, more than half of the cases of malignant glioma showed Lip. This concept stemmed from the fact that the glioblastoma cases with Lip (Nos. 8, 17 and 21) showed a high positive cell rate of Sudan-II staining and MIB-1 index. It is indicated that the biological activity and the proliferating capacity of tumors are higher at those areas, vascular proliferation lags behind, and many cells utilize lipid droplets as a source of energy by absorbing them.

Ganglioneuroblastoma showed a similar trend. Contrarily, there was a case (No. 20) of an anaplastic astrocytoma that showed a high Cho/Cr ratio, about three times as high as the normal value, and was suspected of having a high tumor activity from an MIB-1 index of 16.3%, but did not show Lip and only a low positive cell rate of Sudan-II staining of 4.9%. This indicated that the early stage of tumor growth when the proliferating capacity of the tumor was high, but it was not with an inadequate blood supply.

In metastatic brain tumor and malignant lymphoma, Lip was observed in a higher incidence. These are malignant tumors with high activity as indicated by the MIB-1 index. Commonly, metastatic brain tumors growth rapidly and cause central necrosis earlier, and lipid droplets also appear in malignant lymphomas. However, one case without Lip was encountered in a metastatic brain tumor. Case No. 1 was a case in which a tumor was detected at a relatively early stage, because pathological necrosis was observed in spite of a solid tumor shown on the MRI[20,21]. This was probably due to the voxel setting problem of the ^{1}H-MRS and a problem of accuracy. It was detected by the NAA because it is in the normal brain tissue.

There was no correlation between Sudan-II staining and the MIB-1 index for a meningioma. But there were 2 cases with no necrosis and no positive Sudan-II staining despite the appearance of Lip. There are the possibility that there were lipid producing cells and benign microcyst which were degenerated in this tumors. Moreover it remains difficult to identify several subtypes of meningioma with ^{1}H-MRS[22]. Conversely, in cases with necrosis